

## DATA-DRIVEN SIMPLE THERMAL MODELS: THE RADIATOR-GAS CONSUMPTION MODEL

Vanda Dimitriou\*, Steven K. Firth, Tarek M. Hassan, Tom Kane and Michael Coleman  
School of Civil and Building Engineering, Loughborough University, Leicestershire  
LE11 3TU, United Kingdom  
\*V.Dimitriou@lboro.ac.uk

### ABSTRACT

A simple data-driven Lumped Parameter thermal model is developed linking the radiator surface temperature to the whole house gas consumption using operational data collected from a real house. The indoor room air temperatures, the radiator surface temperatures and the whole house gas consumption are used as input data. The model parameters are estimated using the Ordinary Least Squares technique. Results show that an improved fit can be achieved by excluding data points for which gas consumption is being used for purposes other than space heating using a lower threshold ( $T_{r,pred} - T_{r,meas}$ ) of  $1^{\circ}\text{C}$  during the model calibration. Finally, the model is applied to disaggregate the gas consumption data that are linked to space heating from the original whole house gas consumption at half-hourly intervals.

### INTRODUCTION

As advanced equipment is emerging in the domestic sector (e.g. Smart Home equipment), we are faced with a wealth of operational data which is often unused. Appropriate thermal modelling techniques need to be identified that are able to best make use of the real-time performance data arising from in-home sensors in order to reduce heating energy demand, better inform maintenance and retrofit actions and help towards the reduction of the performance gap (De Wilde, 2014). The Lumped Parameter method has proven popular in the field of data-driven statistical modelling (Andersen et al., 2000, Déqué et al., 2000, Bacher and Madsen, 2011, Fouquier et al., 2013 and Dimitriou et al., 2014). The term ‘Lumped’ refers to the grouping of multiple layers of the building elements into a single node. The Lumped Parameter modelling technique, originally developed in the 1970s, has found multiple applications throughout the years (Tindale, 1993, Lombard and Mathews, 1999, Gouda et al. 2002 and Xu and Wang, 2008). The Lumped Parameter models have been extensively used to represent parts of the heating system and, in particular, to model the radiator surface temperature and heat output to its surrounding environment.

A Lumped Parameter model is used in the software ANSYS® FLUENT Academic Research to represent

the radiator surface by using a non-constant heat transfer coefficient that accounts for the variability of the heat output due to different boundary conditions. Gouda et al. (2000) describe the heat emitted through a radiator by dividing the emitter system in two connected subsystems; the first subsystem relates to the water flow through the radiator panel; the second subsystem refers to the heat transferred from the water to the radiator material and subsequently to the room air node. In a similar approach, Tahersima et al. (2011) calculated the power from the radiator due to convection by separating the radiator into a number of elements and by using multiple measurements of the radiator temperature. Liao and Dexter (2004) and more recently Maivel and Kurnitski (2014) explain that the thermal dynamics of the radiator are governed by the power supplied to the radiator, the power emitted through radiation and the power emitted through convection. Underwood (1999) used a non-linear model to describe the output of a hot water heat emitter describing both natural convection and heat exchange due to long-wave radiation. The radiator model used by Andersen et al. (2000) relates the heat output of the radiator to the supply and return water temperatures of the flow and the room air temperature using a constant ‘c’ and assuming a rather constant flow. Similarly, in their work on dynamic modelling of a room Yu and Paassen (2004) introduce an additional term for the radiative heat exchange from the radiator to other solid surfaces (e.g. wall). A heat balance equation for the Thermostatic Radiator Valves (TRV) has been proposed by Xu et al. (2008) which relates the temperature difference of the TRV sensor to the temperature difference between the sensor and the room air by using a heat transfer coefficient ‘K’. Finally, Garbai and Barna (2005) in their work on modelling the non-steady-state conditions in a gas boiler heated room link the radiator heat output to the energy output from the boiler using an equation describing the heat balance of the heat circuit.

This paper focuses on developing a simple data-driven Lumped Parameter thermal model linking the radiator surface temperature to the whole house gas consumption using operational data collected from a real house. The model parameters are calculated and the goodness of fit to the monitored data is assessed. By excluding time-stamps of assumed mixed-use gas

consumption (gas used for purposes other than heating, such as cooking and Domestic Hot Water) the model fit is improved. Finally the model is used to disaggregate the gas consumption data linked to space heating from the original whole house gas consumption at half-hourly intervals.

## CASE STUDY: A HOME IN LOUGHBOROUGH

An initial exploration of the selected modelling method was realised for a typical UK domestic building. The building has a varying occupancy of up to three people and thus the applicability of the modelling methods to real-life households was investigated. In contrast to experimental buildings and laboratory environments where most of the parameters can be controlled and adapted, this study explores the uncertainties involved in real domestic buildings where occupant behaviours and heating practices play a significant role in the total energy performance. In this section a description of the building is given, followed by a description of the measurement equipment and the data collected.

### **House description**

The house is a two-storey traditional semi-detached house built in the early 1970s, situated in Loughborough, UK. In Figure 1 the floorplans of the house are given along with the openings and radiator placement. The groundfloor consists of an entrance hallway, a living room, a kitchen-dining room and the first floor has three bedrooms and a family bathroom. The total floor area amounts to approximately 78m<sup>2</sup>. The external construction consists of insulated cavity walls and double glazed openings. The floor to ceiling height is 2.4m. The central heating system is a typical wet system with radiators and a central boiler. The condensing combi boiler, model of 2013, is using gas as its primary fuel. There are seven radiators in the house, five of which are single-surface radiators and the remaining two (in the kitchen-dining room and the living room) are double-surface radiators. The living room is also equipped with a solid fuel stove (woodburner).

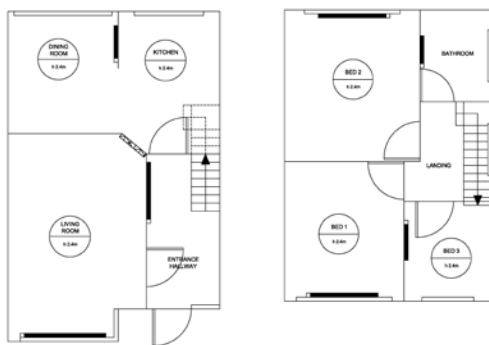


Figure 1 Floorplans of groundfloor (left) and first floor (right) with radiator positioning (in black blocks)

## **Measurement equipment and data collected**

Table 1 summarises the measured data and provides further details on the time intervals and equipment used. Hobo temperature data loggers were placed in each room at a head high level away from obstacles, direct solar radiation, currents and heat sources (when possible) to capture the internal air temperature ( $T_i$ ). For the monitoring of the radiator surface temperature ( $T_r$ ) One-wire iButton standalone sensors were selected for their small size and their advantage of non-intrusive attachment to the surfaces due to the lack of wiring. The capability of the iButton sensors to monitor the temperature of a surface has been already proven in the field of thermophysiology by Van Marken Lichtenbelt et al. (2006) and more recently by Smith et al. (2010) in their research work on evaluating the human skin temperature using iButtons. An external company was employed to monitor the whole house gas consumption ( $Q_h$ ) at a half-hourly interval. The monitoring lasted for a 8-week time-period during the 2014 heating season; starting the 1<sup>st</sup> of February and ending the 28<sup>th</sup> of March 2014.

Table 1  
Operational data captured, the equipment used and the time interval used

Monitoring of	Positioning	Equipment used	Interval (min)
Internal air temperature $T_i$ (°C)	One in each room including hallways and landing	HOBO U12 - HOBO Pendants	30
Radiator surface temperature $T_r$ (°C)	One on each radiator	One-wire iButtons	30
Gas consumption $Q_h$ (m <sup>3</sup> )	Whole house, cumulative measurements <sup>1</sup>	Automated meter reader	30

<sup>1</sup>Conversion factor used for Loughborough, sourced from <http://www.energylinx.co.uk>; 1m<sup>3</sup> equals to 11.363kWh

## THE RADIATOR-GAS CONSUMPTION MODEL

### **Model development**

A simple two-node linear model describing the dynamics between the gas consumption  $Q_h$ , the radiator surface temperature  $T_r$  and the building internal temperature  $T_i$  is developed. The model is used to identify how the radiator surface temperature relates to gas consumption and quantify the energy used for space heating using the main heating system. Figure 2 shows the relevant lumped parameter model taking into account the convective heat transfer between the radiator surface and the indoor air temperature node.

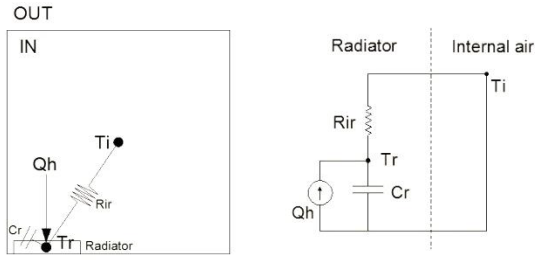


Figure 2 A two dimensional representation of the lumped parameter model (left) and the RC-network/electrical analogy (right)

The differential equations describing the heat transfer occurring at the internal air node at a whole house level are given below:

$$dT_{r,pred} = \left[ \frac{(T_{i,meas} - T_{r,pred})}{C_r R_{ir}} + \frac{\alpha Q_h}{C_r} \right] dt \quad (1)$$

$$dT_{r,pred} = [\alpha(T_{i,meas} - T_{r,pred}) + \beta Q_h] dt \quad (2)$$

where  $T_{i,meas}$  is the non-weighted average of all the room air temperature measurements of the previous time step,  $T_{r,pred}$  is the non-weighted average of all the radiator surface temperature predictions of the previous time step and  $dT_{r,pred}$  is the difference in the radiator surface temperature as predicted by the model.

#### Initial model fit

To calculate the unknown model parameters,  $\alpha$  and  $\beta$ , the Ordinary Least Square (OLS) parameter estimation technique is used (Reddy, 2011).

Table 2 summarises the model results. The parameter values that minimise the Sum of the Squared Errors (SSE) between the measured radiator surface

temperature,  $T_{r,meas}$ , and the predicted radiator surface temperature,  $T_{r,pred}$ , are calculated. The model is calibrated using as input variables all half-hourly interval time-stamps of room air temperature,  $T_i$ , and gas consumption,  $Q_h$ . The Root Mean Squared Error (RMSE) i.e. the mean error between the predicted and measured radiator surface temperature per time-stamp ( $^{\circ}\text{C}$ ) is also calculated.

Table 2

Model parameters and goodness of fit metrics			
$\alpha$	$\beta$	SSE (based on 2688 measurements)	RMSE ( $^{\circ}\text{C}$ )
0.43	1.99	59802.60	4.72

Figure 3 presents the model output,  $T_{r,pred}$ , the measured radiator surface temperature,  $T_{r,meas}$ , and the gas consumption input variable values,  $Q_h$ , against time. It is clear that the model under-predicts the radiator surface temperature (a difference of about  $5^{\circ}\text{C}$ ) during most of the daily peaks throughout the 8-week time-period. Occasionally the model over-predicts, driven by the very high gas consumption of the relative time-stamps. This was expected as the gas consumption data used to calculate the radiator surface temperature included the gas consumption used for other purposes such as Domestic Hot Water (DHW) and cooking. The inclusion of gas consumption for uses other than space heating through the central heating system during the model calibration using the OLS technique results in unreasonable temperature peaks, driving the model to under-predict for the rest of the time-period in order to compensate for the increased error.

To further explore how the model predicts Figure 4

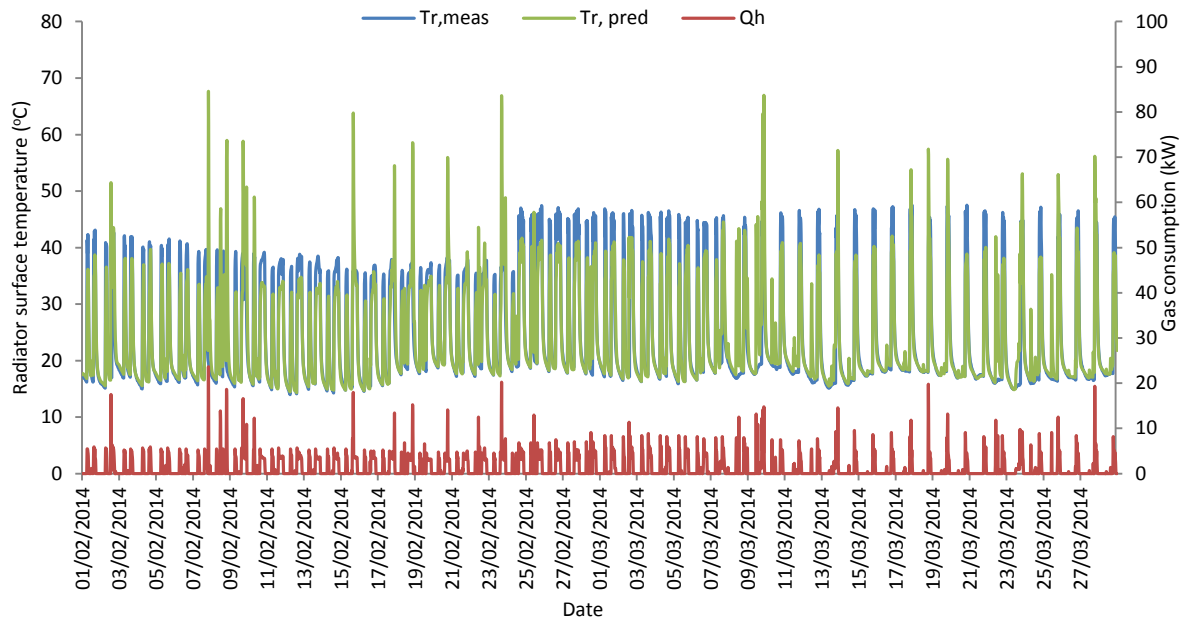


Figure 3 Radiator surface temperature as measured  $T_{r,meas}$  ( $^{\circ}\text{C}$ ) and as predicted  $T_{r,pred}$  ( $^{\circ}\text{C}$ ) using the total gas consumption data  $Q_h$  (kW) for the 8-week period of the 2014 heating season.

presents the model output,  $T_{r,pred}$ , the measured surface temperature,  $T_{r,meas}$ , and the input gas consumption,  $Q_h$ , against time for an example day (the 19<sup>th</sup> of February 2014). The model under-predicts the radiator temperature (within a range of about 3°C to 6°C) when the heating is on and over-predicts the radiator temperature at midday when the heating should be off. This is a clear indication that the gas consumption presented between 11:00 and 14:00 is used for purposes other than space heating causing the model to predict an increased radiator surface temperature when there is no space heating through the central heating system.

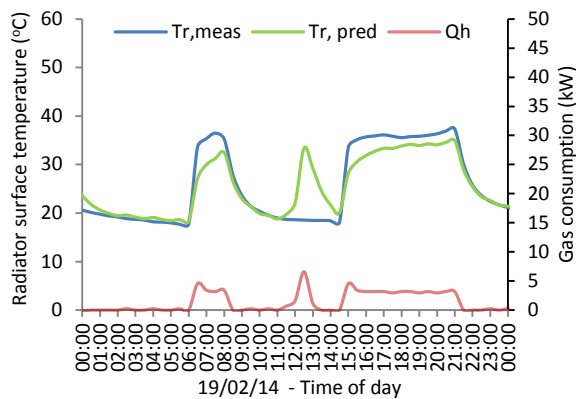


Figure 4  $T_{r,meas}$  (°C),  $T_{r,pred}$  (°C) using the total gas consumption data  $Q_h$  (kW) for the 19<sup>th</sup> of February.

Another example day of the 8-week time-period (the 19<sup>th</sup> of March 2014) is presented in Figure 5. In this case, the model both under-predicts and over-predicts during the time-period that the radiator temperatures are highest, presenting a peak in the surface temperature that cannot be related to the measured radiator temperature. This could be an indication that during the space heating period (18:00 and 22:00) gas consumption is being used to serve for additional purposes, misleading to even higher peaks of radiator surface temperature than the expected.

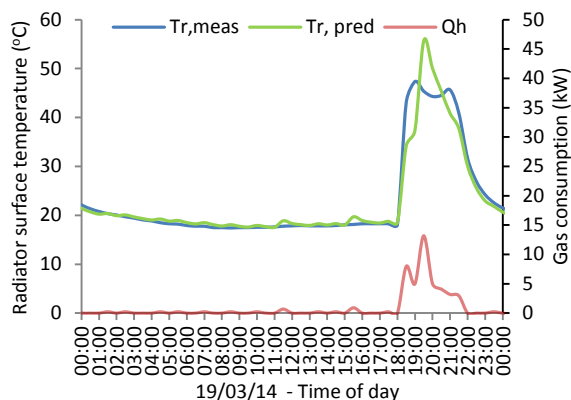


Figure 5  $T_{r,meas}$  (°C),  $T_{r,pred}$  (°C) using the total gas consumption data  $Q_h$  (kW) for the 19<sup>th</sup> of March.

Figure 6 is a scatter plot of the model output,  $T_{r,pred}$ , against the measured surface temperature,  $T_{r,meas}$ ,

which can be used to assess how well the model predicts across the whole 8-week time-period. A perfect fit between the predicted and measured data would be indicated by a perfect positive linear association. In this case, all the data points would fall perfectly on the black line. However, having already explored the time-plots, a less than perfect fit should be expected. Indeed, while most of the data-points fall on the black line indicating an adequate fit, a significant number of data-points deviates from the linear association. With the y axis indicating the value of the predicted temperatures and the x axis the relative measured values, any values falling above the black line indicate an instance of overprediction and all values below the line should be linked to underprediction. The RMSE value of 4.72°C from Table 2 can be used as an indication of how scattered the data are from the black line. The better the linear association, the closer the RMSE value is to zero.

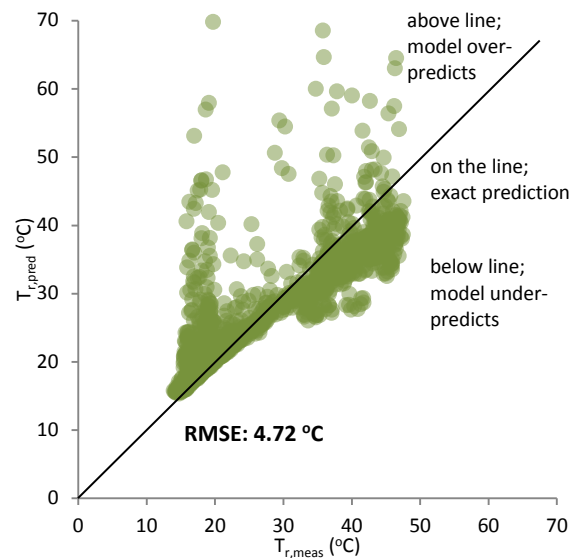


Figure 6  $T_{r,meas}$  (°C) against  $T_{r,pred}$  (°C) indicating how well the model fits and all the instances of over-/under-prediction.

In this section the model parameters were calculated using all half-hour time-stamps of the input variable  $Q_h$ . The results showed that the inclusion of gas used for purposes other than space heating (through the central heating system) in the calculation of the predicted radiator surface temperature resulted in an inadequate fit to the measured data. In particular, the model over-predicted the radiator temperature when gas consumption was used for multiple purposes and under-predicted throughout the rest of the time-period.

In the next section, to improve the model fit, selected time-stamps of the 8-week time-period for which gas consumption is causing temperature overprediction are excluded from the model calibration.

#### Model calibration using selected time-stamps

In order to define overprediction, an error threshold need to be chosen above which gas data values are

assumed to incorporate gas used for multiple purposes and therefore should be excluded from the model calibration. This serves to ensure that time-stamps for which the model is overpredicting due to other reasons, such as inadequate initial parameter values, are not attributed to mixed gas consumption and, therefore, unnecessarily removed from the input data.

In Table 3 different error thresholds between the predicted and measured radiator surface temperature are being explored. Using a macro written in VBA Excel, time-stamps for which the error ranges from 0°C to the maximum identified difference (e.g. 60°C) are gradually excluded from the model calibration and the model parameter values and model fit metrics are calculated. The number of measurements used for the model calibration is taken into account. The threshold for which the best model fit is achieved, i.e. the threshold for which the lowest RMSE value is presented, is considered to provide adequate calculation of the model parameter values. In this case, excluding all time-stamps for which  $T_{r,pred} - T_{r,meas} > 1^\circ\text{C}$  resulted in the lowest RMSE (2.08°C). The proportion of gas usage data excluded during calibration for each threshold is listed in the last two columns. The threshold of 1°C resulted in the exclusion of 23.73% of all gas usage data (including the time-periods when gas consumption is zero) and 10.97% of gas data excluded for the time-periods during which heating was on. Ensuring that an adequate proportion of gas usage data when heating is on is used during calibration is crucial to ensure that the parameter estimation is based on these important time-periods when most information on space heating is available.

Table 3

Exploring different thresholds for data exclusion from the model calibration

$T_{r,pred} - T_{r,meas} >$ threshold (°C)	$\alpha$	$\beta$	RMSE on included time-stamps	Gas data excluded
60	0.43	1.99	4.72	0.00%
50	0.43	1.99	4.72	0.00%
40	0.44	2.07	4.56	0.14%
30	0.46	2.17	4.39	0.35%
20	0.52	2.58	3.61	1.84%
10	0.59	3.08	2.61	4.73%
9	0.59	3.07	2.60	4.87%
8	0.58	3.08	2.53	5.51%
7	0.58	3.09	2.46	6.14%
6	0.59	3.13	2.37	6.99%
5	0.58	3.14	2.28	8.26%
4	0.58	3.15	2.19	10.17%
3	0.58	3.19	2.10	12.57%
2	0.58	3.19	2.09	14.34%
1	0.58	3.22	2.08	23.73%
0	0.58	3.24	2.22	52.19%

Figure 7 presents the time-stamps excluded during calibration when using the threshold of 1°C. There are 336 time-stamps excluded out of the 2688 original time-stamps with 76 of them (in red) relating to the time-period when the heating is on. The red data points suggest that gas is used for both space heating and other purposes whereas the green data points suggest that gas is used only for other purposes. Most of the instances when space heating through the central heating system is used in conjunction with other activities requiring gas usage appear late in the afternoon and during the evening and in particular between 15:30 and 21:30. This result suggests that in this dwelling cooking and DWH are most commonly used during these hours.

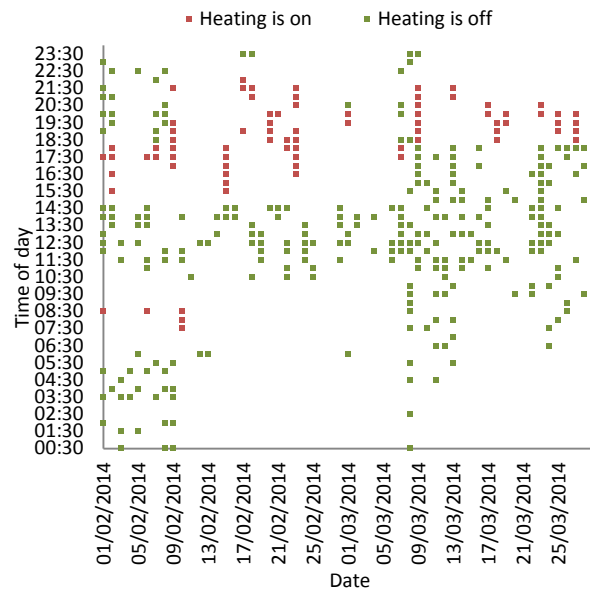


Figure 7 Time-stamps excluded during calibration when a threshold  $T_{r,pred} - T_{r,meas} > 1^\circ\text{C}$  is selected.

Figure 8 presents the model output,  $T_{r,pred}$ , and the measured radiator surface temperature,  $T_{r,meas}$ , for the 8-week time-period. The time-stamps for which the  $T_{r,pred} - T_{r,meas} > 1^\circ\text{C}$  condition is satisfied are excluded from the model calibration and are indicated in the graph by a grey vertical line. All of the peaks that deviate more than +1°C from the measured temperature have been excluded from the calibration. The model fit is significantly improved when compared to the initial fit of Figure 3. By excluding all the unnecessary peaks the model achieves a much better fit during the time-periods included in the calibration procedure.

Figure 9 presents the model output,  $T_{r,pred}$ , the measured surface temperature,  $T_{r,meas}$ , and the excluded time-stamps for the same day as Figure 4 (the 19<sup>th</sup> of February 2014). Four time-stamps have been excluded from the calibration for this day. The model fit has improved significantly during the time-periods when the heating is on. The model is still



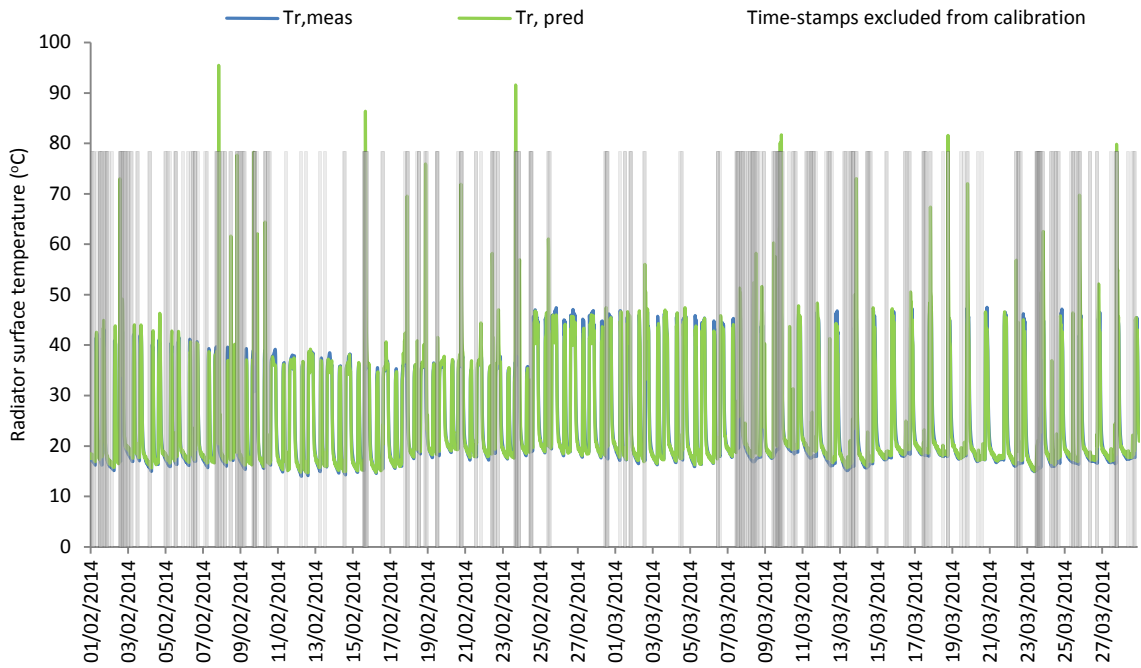


Figure 8 Radiator surface temperature as measured  $T_{r,meas}$  ( $^{\circ}C$ ) and as predicted  $T_{r,pred}$  ( $^{\circ}C$ ) excluding selected time-stamps ( $T_{r,pred}-T_{r,meas}>1^{\circ}C$ ) for the 8-week period of the 2014 heating season.

over-predicting during the 11:00 to 14:00 time-period due to the gas consumption for purposes other than space heating. To remove these peaks the gas consumption data would need to be disaggregated and the gas consumption for other purposes removed.

Similarly, Figure 10 presents the model output,  $T_{r,pred}$ , the measured surface temperature,  $T_{r,meas}$ , and the excluded time-stamps for the same day as Figure 5 (the 19<sup>th</sup> of March 2014). Again, four time-stamps have been removed from the model calibration, two instances related to gas usage when heating is off (at 11:30 and 15:30) and the remaining two related to gas consumption used for other purposes when heating is on (at 19:30 and 20:00). The model fit is improved from the initial model fit during the hours

18:00-19:00 and 20:30-22:00 when the heating is on and gas is not being used for other purposes other than space heating.

Finally, Figure 11 is a scatter plot of the model output,  $T_{r,pred}$ , against the measured surface temperature,  $T_{r,meas}$ , which can be used to assess how well the model predicts across the whole 8-week time-period, same as Figure 6. This scatter plot uses only the selected time-stamps for calibration. The model fit for the selected data points is significantly improved, with the majority of the data along the black line indicating a stronger linear association. This was also reflected in the respective RMSE value of Table 3 of  $2.08^{\circ}C$ , an improvement of  $2.64^{\circ}C$  from the initial model.

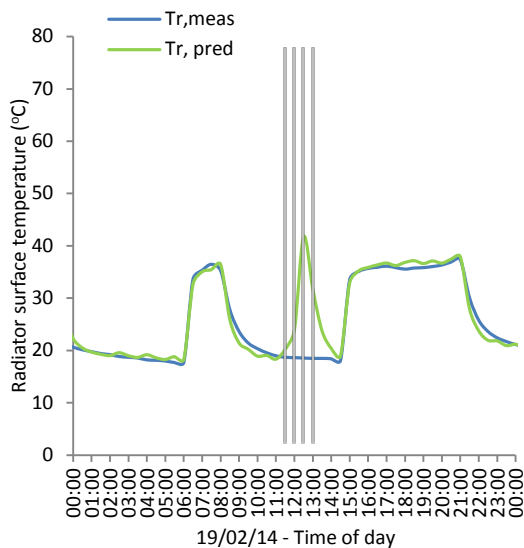


Figure 9  $T_{r,meas}$  ( $^{\circ}C$ ),  $T_{r,pred}$  ( $^{\circ}C$ ) excluding selected time-stamps for the 19<sup>th</sup> of February.

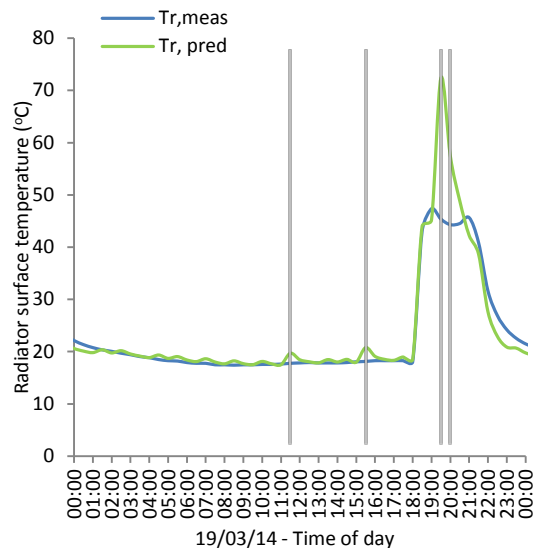


Figure 10  $T_{r,meas}$  ( $^{\circ}C$ ),  $T_{r,pred}$  ( $^{\circ}C$ ) excluding selected time-stamps for the 19<sup>th</sup> of March.

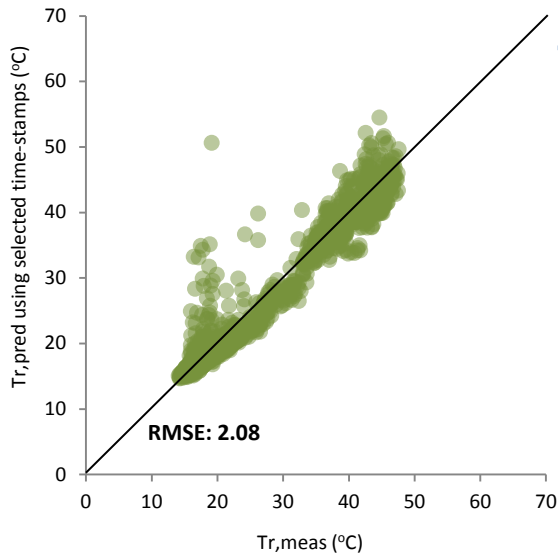


Figure 11  $T_{r,meas}$  ( $^{\circ}C$ ) against  $T_{r,pred}$  ( $^{\circ}C$ ) indicating how well the model fits for selected time-stamps.

### Application of the model

Once the linear model is calibrated and the parameter values calculated, the model can be used to select the gas consumption data that are linked to space heating only. To achieve that, the first step is to replace the predicted values of radiator surface temperature for the time-stamps that were previously excluded from the calibration procedure with the measured temperature data. This creates a new time series of radiator surface data,  $T_{r,gas}$ . The second step is to reverse the modelling procedure. Using  $T_{r,gas}$  and the parameter values  $\alpha$  and  $\beta$  as input data the gas consumption related to space heating can be calculated.

Figure 12 shows how the gas consumption data have been corrected and the time-stamps of correction for one example day (the 19<sup>th</sup> of February 2014). Four

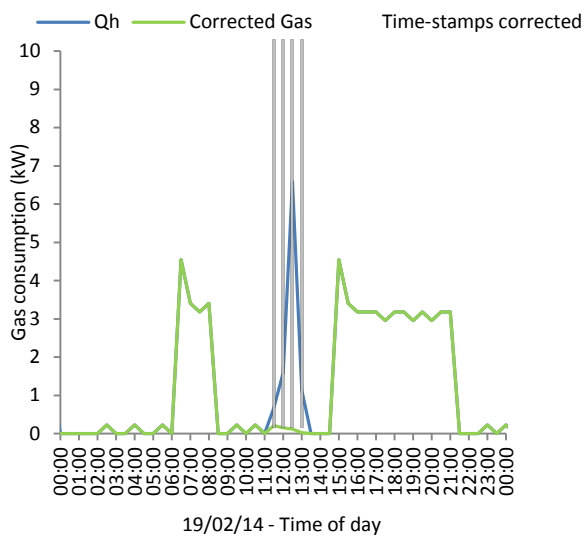


Figure 12 The original gas consumption data,  $Q_h$ , the corrected gas consumption data and the time-stamps for which corrections occurred for one day.

gas data points have been corrected and the peak of gas consumption between 11:00 and 13:30 which is not related to space heating has been removed. The gas consumption data during the time-periods that the heating is on remain the same as the original gas data as there was no indication of mixed gas usage.

Figure 13 shows another example of gas data correction for a different day (the 19<sup>th</sup> of March 2014). In this case there are four instances of gas data correction, two of which during the time-period that the heating is on. The gas data at this point is calculated to match the need for space heating reducing the gas consumption peak from 13.18kW down to 4.89kW. This implies that 8.29kW of gas consumption served for purposes other than space heating.

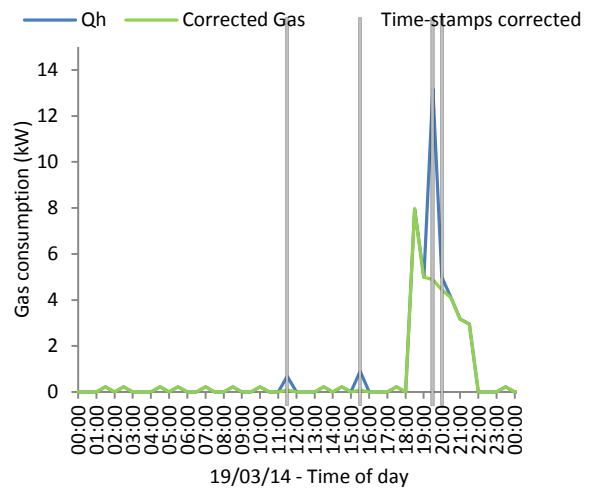


Figure 13 The original gas consumption data,  $Q_h$ , the corrected gas consumption data and the time-stamps for which corrections occurred for one day.

Finally, Figure 14 shows the original gas consumption data (x axis) against the corrected gas consumption data for space heating (y axis). All values across the diagonal of the graph are gas consumption data that maintained their original values. All points beneath the diagonal relate to data that had to be completely removed (data falling along the x axis) or data that needed to be reduced.

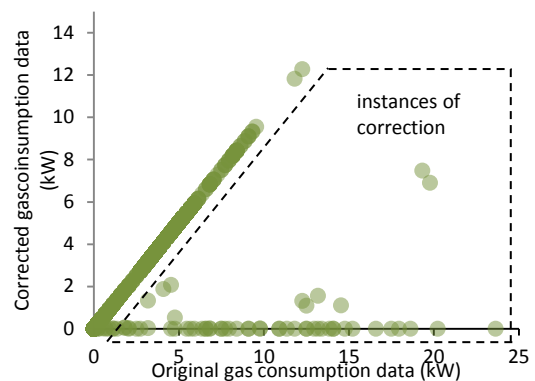


Figure 14 Original and corrected for space heating gas consumption data as calculated using the calibrated linear model

## CONCLUSIONS

A simple data-driven Lumped Parameter thermal model has been developed linking the radiator surface temperature to the whole house gas consumption using operational data collected from a real house. The whole house gas consumption data, consisting of gas used for space heating as well as other purposes, has been used to drive the model. Due to the end uses for gas consumption, the model fit was inadequate, under-predicting when space heating was on and over-predicting when gas was used for other purposes. A critical examination of different thresholds to remove the time-stamps for which the model over-predicted during calibration showed that a threshold of 1°C could provide the best model fit (RMSE of 2.08°C, of 2.64°C lower than the initial model fit). Finally, the model was used to select the gas consumption data that are linked to space heating only, by correcting the original whole house gas consumption at the time-stamps where gas usage for other purposes was identified.

This work is of significant interest to the building physics community for identifying models for domestic buildings with in-home sensors based on real-time data and to the UK government for promoting smart metering as an energy efficiency strategy and for bridging the performance gap. Further work will expand the findings of this paper in a study of 12 UK homes.

## NOMENCLATURE

$T_{r,pred}$	is the radiator surface temperature as predicted by the model ( °C)
$T_{r,meas}$	is the radiator surface temperature as measured ( °C)
$T_{i,meas}$	is the indoor air temperature ( °C)
$Q_h$	is the gas consumption (W)
$C_r$	is the heat capacitance of the radiator (W/°C)
$R_{ir}$	is the thermal resistance between the radiator and the air (°C/W)
$a$	is a factor of boiler efficiency and pipe heat losses
$\alpha$	is the convective heat transfer coefficient
$\beta$	is the gas consumption coefficient

## ACKNOWLEDGEMENTS

This work has been carried out as part of the REFIT project ('Personalised Retrofit Decision Support Tools for UK Homes using Smart Home Technology', £1.5m, Grant Reference EP/K002457/1). For more information see: [www.epsrc.ac.uk](http://www.epsrc.ac.uk) and [www.refitsmarthomes.org](http://www.refitsmarthomes.org)

## REFERENCES

Andersen, K.K., Madsen, H., Hansen, L.H., 2000. Modelling the heat dynamics of a building using stochastic differential equations. *Energy and Buildings*; 31(1), 13-24.

- Bacher, P., Madsen, H., 2011. Identifying suitable models for the heat dynamics of buildings. *Energy and Buildings* 2011; 43(7), 1511-1522.
- Déqué, F., Ollivier, F., Poblador, A., 2000. Grey boxes used to represent buildings with a minimum number of geometric and thermal parameters. *Energy and buildings*; 31(1), 29-35
- De Wilde, P., 2014. The gap between predicted and measured energy performance of buildings: A framework for investigation. *Automation in Construction*; 41, 40-49.
- Dimitriou, V, Firth, S.K., Hassan, T.M., Kane, T., Fouchal, F., 2014. Developing suitable thermal models for domestic buildings with Smart Home equipment. The Bartlett: UCL Faculty of the Built Environment Institute for Environmental Design and Engineering: IBPSA-England;
- Fouquier, A., Robert, S., Suard, F., Stephan, L., Jay, A., 2013. State of the art in building modelling and energy performances prediction: A review. *Renewable and Sustainable Energy Reviews*; 23, 272-288.
- Garbai, D.L., Barna, D.L., 2006. Modelling of non-steady-state conditions in a gas boiler heated room. *energy*, 10, 11.
- Gouda, M.M., Danaher, S., Underwood, C.P., 2000. Low-order model for the simulation of a building and its heating system. *Building Services Engineering Research and Technology*, 21(3), 199-208.
- Gouda, M.M., Danaher, S., Underwood, C.P., 2002. Building thermal model reduction using nonlinear constrained optimization. *Building and Environment*; 37(12), 1255-1265.
- Liao, Z., Dexter, A.L., 2004. A simplified physical model for estimating the average air temperature in multi-zone heating systems. *Building and environment*, 39(9), 1013-1022.
- Lombard C, Mathews EH. 1999. A two-port envelope model for building heat transfer. *Building and environment*; 34(1), 19-30.
- Maivel, M., Kurnitski, J., 2014. Low temperature radiator heating distribution and emission efficiency in residential buildings. *Energy and Buildings*, 69, 224-236.
- Reddy, T.A., 2011. *Applied data analysis and modeling for energy engineers and scientists*. Springer Science & Business Media.
- Smith, A.H., Crabtree, D.R., Bilzon, J.L., Walsh, N.P., 2010. The validity of wireless iButtons® and thermistors for human skin temperature measurement. *Physiological Measurement*, 31(1), 95.
- Tahersima, F., Stoustrup, J., Rasmussen, H., 2011. Eliminating oscillations in trv-controlled hydronic radiators. In *Decision and Control and European Control Conference (CDC-ECC)*, 2011 50th IEEE Conference on (pp. 4407-4412). IEEE.
- Tindale, A., 1993. Third-order lumped-parameter simulation method. *Building Services Engineering Research and Technology*; 14(3), 87-97.
- Underwood, C.P., 1999. *HVAC control systems: Modelling, analysis and design*. Routledge.
- Van Marken Lichtenbelt, W.D., Daanen, H.A., Wouters, L., Fronczek, R., Raymann, R.J., Severens, N.M., Van Someren, E.J., 2006. Evaluation of wireless determination of skin temperature using iButtons. *Physiology & Behavior*, 88(4), 489-497.
- Xu, B., Fu, L., Di, H., 2008. Dynamic simulation of space heating systems with radiators controlled by TRVs in buildings. *Energy and buildings*, 40(9), 1755-1764.
- Xu, X., Wang S., 2008. A simplified dynamic model for existing buildings using CTF and thermal network models. *International Journal of Thermal Sciences*; 47(9), 1249-1262.
- Yu, B., Van Paassen, A.H.C., 2004. Simulink and bond graph modeling of an air-conditioned room. *Simulation Modelling Practice and Theory*, 12(1), 61-76.